# Pre-Steady-State Study of Recombinant Sesquiterpene Cyclases†

Jeffery R. Mathis,‡ Kyoungwhan Back,§ Courtney Starks,|| Joe Noel,|| C. Dale Poulter,*,‡ and Joseph Chappell*,§

*Department of Chemistry, University of Utah, Salt Lake City, Utah 84112, Plant Physiology/Biochemistry/Molecular Biology Program, University of Kentucky, Lexington, Kentucky 40546-0091, and Structural Biology Laboratory, Salk Institute, San Diego, California 92037*

*Received December 9, 1996; Revised Manuscript Received May 2, 1997*⊗

ABSTRACT: An *Escherichia coli* expression system was used to generate hexahistidyl-tagged plant sesquiterpene cyclases, which were readily purified by a single affinity chromatographic step. Genes for *Hyoscyamus muticus* vetispiradiene synthase (HVS), a chimeric 5-epi-aristolochene synthase (CH3), and a chimeric sesquiterpene cyclase possessing multifunctional epi-aristolochene and vetispiradiene activity (CH4) were expressed in bacterial cells, which resulted in the sesquiterpene cyclases accumulating to 50% of the total protein and 35% of the soluble protein. From initial velocity experiments, the Michaelis constant for HVS was 3.5 $\mu$M, while CH3 and CH4 exhibited smaller values of 0.7 and 0.4 $\mu$M, respectively. Steady-state catalytic constants were from 0.02 to 0.04 $s^{-1}$. A combination of pre-steady-state rapid quench experiments, isotope trapping experiments, and experiments to measure the burst rate constant as a function of substrate concentration revealed that turnover in all three cyclases is limited by a step after the initial chemical step involving rupture of the carbon−oxygen bond in farnesyl diphosphate (FPP). Rate constants for the limiting step were 10−70-fold smaller than for the initial chemical step. Dissociation constants for the enzyme−substrate complex (20−70 $\mu$M) were determined from the pre-steady-state experiments and were significantly larger than the observed Michaelis constants. A mechanism that involves an initial, rapid equilibration of enzyme with substrate to form an enzyme−substrate complex, followed by a slower conversion of FPP to an enzyme-bound hydrocarbon and a subsequent rate-limiting step, is proposed for the three enzymes. Interestingly, the multifunctional chimeric enzyme CH4 exhibited both a tighter binding of FPP and a faster conversion of FPP to products than either of its wild-type parents.

Sesquiterpene cyclases are a family of enzymes that catalyze the conversion of the acyclic substrate farnesyl diphosphate (FPP)[1] to a variety of cyclic sesquiterpenes. Cane (1985) estimated that over 200 different sesquiterpene carbon skeletons exist in nature and has emphasized the important role that the cyclase enzymes must play in establishing this diversity. Experimental evidence detailing partial enzymatic steps catalyzed by sesquiterpene cyclases and related monoterpene cyclases has included reports on the initial ionization of FPP (Cane, 1990; Wheeler & Croteau, 1987), isomerization of FPP to its allylic isomer nerolidyl diphosphate, cyclization of the alicyclic sesquiterpene moiety by an intramolecular electrophilic attack on distal double bonds (Cane, 1990; Croteau, 1987; Cane & Tsantrizos, 1996), internal cyclization (Cane et al., 1990a), hydride shifts, and methyl migrations (Cane, 1990; Cane et al., 1990a). Currently, mechanistic questions about the roles of the cyclase proteins themselves in mediating these intricate reactions are being pursued (Cane et al., 1995a,b; Back & Chappell, 1996).

In Solanaceous plants, sesquiterpene cyclases catalyze key regulatory steps in the synthesis of antimicrobial sesquiterpenes (Stoessl et al., 1976; Guedes et al., 1982; Watson & Brooks, 1984; Zook et al., 1992). One example is tobacco 5-epi-aristolochene synthase (TEAS), which catalyzes the cyclization of FPP to two eremophiliane hydrocarbons (bicyclic, two six-membered rings) (Back & Chappell, 1996). The predominant product (>70%) is 5-epi-aristolochene, which subsequently undergoes hydroxylation to give capsidiol (Figure 1) (Whitehead et al., 1989). Another is vetispiradiene synthase (HVS), which converts FPP to a spirane precursor (bicyclic, one five- and one six-membered ring) destined for solavetivone biosynthesis (Whitehead et al., 1990). Cane (1990a) and Whitehead (1990) proposed the mechanism shown in Figure 1 for formation of 5-epi-aristolochene and vetispiradiene. Both enzymes catalyze an electrophilic cyclization of FPP to produce the putative hydrocarbon germacrene A as an enzyme-bound species that is subsequently protonated to initiate a second round of cyclization−rearrangement reactions. The pathways diverge at a penultimate rearrangement step. It is the ability of the two cyclases to control the regiochemistry of this step that dictates whether 5-epi-aristolochene or vetispiradiene is the final product.

Both the TEAS and HVS genes have been cloned and expressed in *Escherichia coli*, and the bacterially expressed enzymes have been used to validate catalytic fidelity as judged by $Ag^+$-TLC, GC, and GC−MS of the reaction products (Back & Chappell, 1996). However, since both enzymes shared a high degree of amino acid identity (77%)

† This work supported by NSF Grant IBN-9408152 (J.C.) and NIH Grants GM21328 (C.D.P.) and GM54029 (J.N.). J.R.M. is a NIH Postdoctoral Fellow (Grant GM17697).

‡ University of Utah.

§ University of Kentucky.

|| Salk Institute.

⊗ Abstract published in *Advance ACS Abstracts,* June 15, 1997.

[1] Abbreviations: BSA, bovine serum albumin; CH, chimeric cyclase; EDTA, ethylenediaminetetraacetate; FPP, farnesyl diphosphate; HVS, *Hyoscyamus muticus* vetispiradiene synthase; TEAS, tobacco 5-epi-aristolochene synthase; $Ag^+$-TLC, argentation−thin layer chromatography; IPTG, isopropyl $\beta$-D-thiogalactopyranoside; SDS−PAGE, sodium dodecyl sulfate−polyacrylamide gel electrophoresis; PCR, polymerase chain reaction; Mopso, 3-(*N*-morpholino)-2-hydroxypropanesulfonic acid; Tris, tris(hydroxymethyl)aminomethane.

S0006-2960(96)03019-X CCC: $14.00 

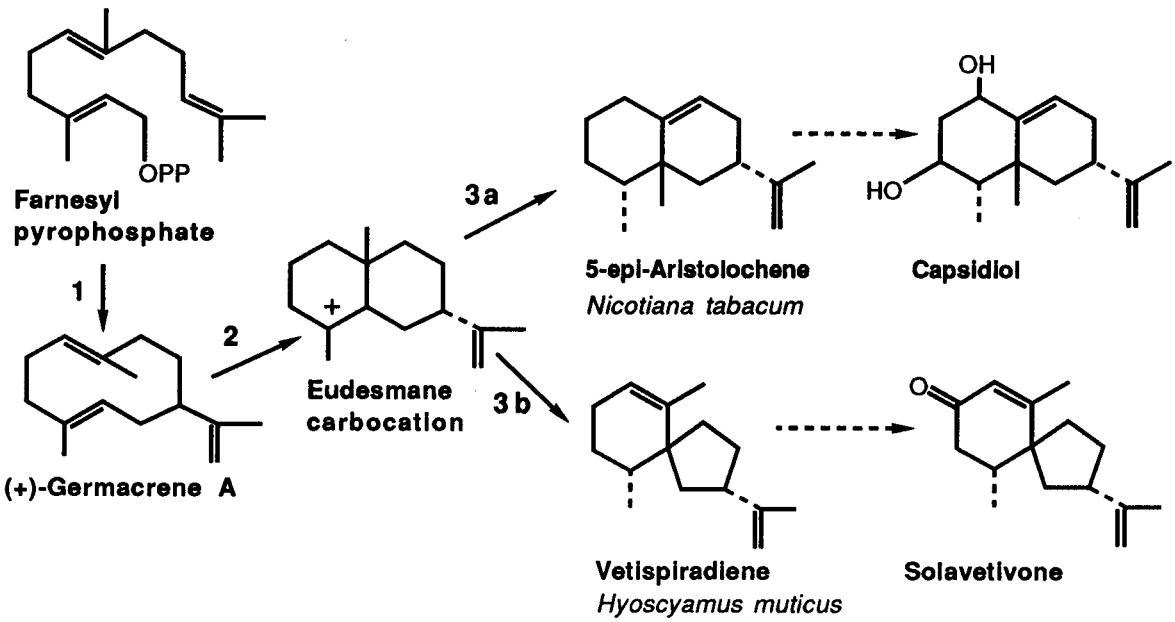


FIGURE 1: Proposed mechanisms for formation of 5-epi-aristolochene and vetispiradiene synthase from tobacco 5-epi-aristolochene synthase (TEAS) and *H. muticus* vetispiradiene synthase (HVS). Steps 1 and 2 are common to both cyclases. Steps 3a and 3b account for the regiochemical differences between TEAS and HVS. Subsequent hydroxylation and oxidation (denoted by dashed arrows) of the sesquiterpene hydrocarbons give rise to the antimicrobial phytoalexins capsidiol and solavetivone [adapted from Cane (1990a) and Whitehead et al. (1990)].

and the amino acid substitutions were more or less evenly distributed throughout the polypeptides, we were unable to identify consensus motifs which might contribute to the unique regioselectivity of the catalysts (Back & Chappell, 1995). Instead, a domain-swapping strategy was developed to map those regions of the cyclase proteins contributing to regiocontrol in the reactions. Unexpectedly, one of the chimeric cyclases catalyzed the synthesis of both the TEAS and HVS reaction products. Further refinement of these chimeric constructs led us to identify two peptide regions responsible for the penultimate rearrangement of reaction products which functioned independently of one another.

Given the pivotal role sesquiterpene cyclases play in plant defense responses and the novelty of the chimeric cyclases in generating reaction products reflective of two parent enzymes, our intent is to determine if the catalytic efficiencies of the chimeric cyclase enzymes are compromised in any way relative to the parent TEAS and HVS enzymes. This paper describes a simple overexpression and purification system for the isolation of substantial amounts of the recombinant cyclase proteins and a detailed kinetic characterization of the enzymes.

## MATERIALS AND METHODS

*Materials*. FPP was synthesized by the method of Davisson et al. (1986). Stock solutions (2−5 mM) made up in 25 mM ammonium bicarbonate were stored at −20 °C until needed. Concentrations were determined by analysis for phosphate (Cassidy et al., 1995). [$^3$H]FPP (17.8 Ci/mmol) was purchased from DuPont-NEN (Boston, MA). All other chemicals were from Sigma (St. Louis, MO) or U.S. Biochemical Corp. (Cleveland, OH) and were used without further purification.

*Construction of Expression Plasmids*. pET28(b) from Novagen (Madison, WI) was used as the expression vector (Figure 2A). This vector contains DNA sequences encoding six histidine residues immediately following several convenient restriction endonuclease sites which were used to construct the pET28(b)-TEAS, -HVS, -CH3, and -CH4 plasmids. For example, the full length 5-epi-aristolochene synthase gene (TEAS) was amplified by PCR using 5′-dGGGAGCTCGAATTCC**ATG**GCCTCAGCAG-CAGTTGCAAACCTAT-3′ as the forward primer (*Eco*RI and *Nco*I restriction sites underlined and the translation start codon in bold), 5′-dGGGCTCGAGAATTTTGATGGAGTC-CACAAG-3′ (*Xho*I site underlined) as the reverse primer, and pBS containing a full length tobacco 5-epi-aristolochene synthase as the template (pBSK-TEAS; Back et al., 1994). The 1668 bp PCR product was digested with *Nco*I and *Xho*I, gel purified, and ligated into the same restriction sites within pET28(b) in-frame with the carboxyl-terminal hexahistidyl-coding sequence. The same strategy was used to generate pET28(b)-HVS, except that the forward primer 5′-dGGC-GAATTCC**ATG**GCCCCAGCTATAGTGATG-3′ (*Eco*RI and *Nco*I restriction sites underlined and the translation start codon in bold), the reverse primer 5′-dCACCTCGAGAATAT-CAATAGAATCCAC-3′ (*Xho*I site underlined), and a pBS template containing the *H. muticus* vetispiradiene synthase gene were used (Back & Chappell, 1995). The chimeric constructs CH3 and CH4 were originally constructed in the pGBT-T19 vector as described by Back and Chappell (1996). pET28(b)-CH3 and -CH4 were constructed using the above-mentioned forward primer employed for construction of pET28(b)-TEAS, the reverse primer used to construct pET28-(b)-HVS, and pGBT-CH3 or pGBT-CH4, respectively, as templates. Constructs were confirmed by limited DNA sequencing of the ligation junctions using the dideoxy chain-termination method (U.S. Biochemical Corp.).

*Bacterial Expression and Purification of Recombinant Cyclases*. Constructs pET28(b)-TEAS, -HVS, -CH3, and -CH4 were transformed into *E. coli* strain BL21(DE3) cells according to the manufacturer's recommendations (Novagen, Madison, WI). One milliliter cultures were used to inoculate 100 mL of Terrific Broth medium (Sambrook et al., 1989)

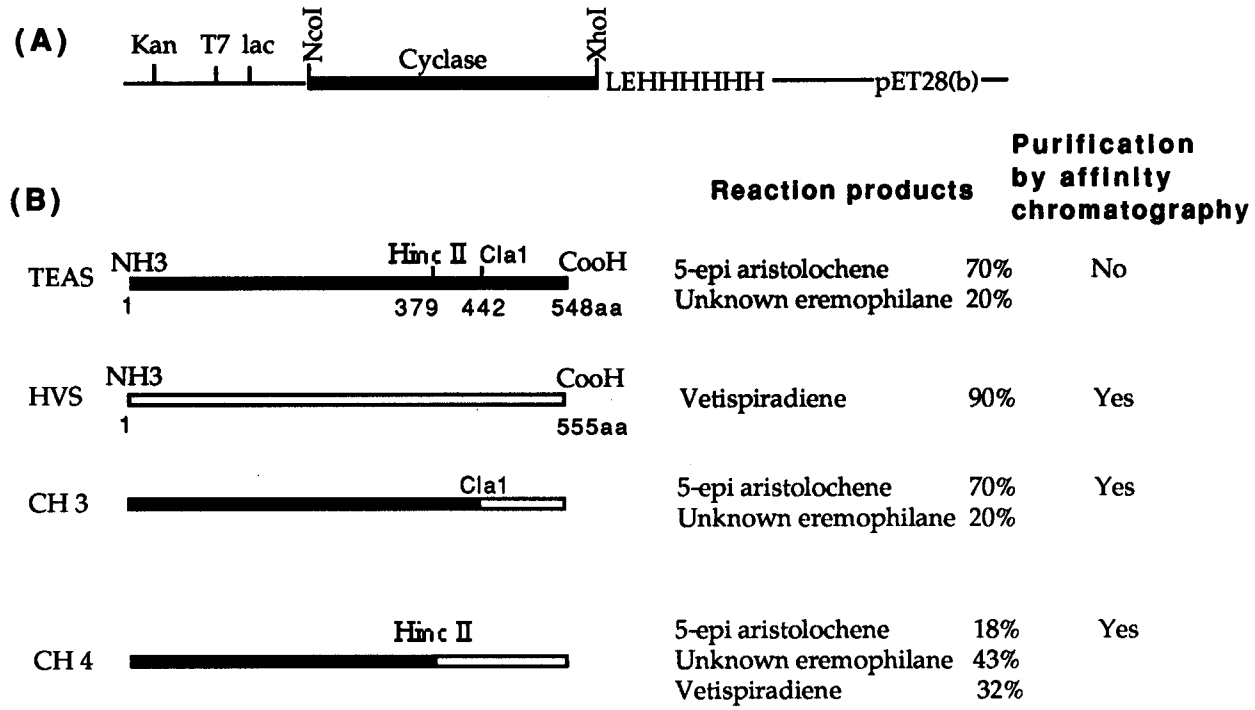


FIGURE 2: Schematic diagram of expression vector pET28b harboring cyclase genes ligated in-frame with DNA sequences coding for hexahistidyl residues (A) and the cyclase genes used for constructing the expression vectors, representative of the enzymic reactions, and an indication of whether the enzyme was successfully purified using affinity ($Ni^{2+}$) chromatography (B). The numbers below endonuclease restriction sites indicate the positions of amino acids within the cyclase polypeptides. Relative amounts of sesquiterpene products (percent) in the reaction mixtures (Back & Chappell, 1996).

containing 50 $\mu$g/mL kanamycin and incubated at 37 °C until $A_{600}$ reached 1.0. After the addition of 0.1 mM IPTG, the cultures were grown at 27 °C for 5 h. The cells were then collected by centrifugation (5000*g* for 5 min at 4 °C), resuspended with 3−5 mL of binding buffer (His-Bind Kit, Novagen), and incubated on ice for 30 min with 3−5 mg of lysozyme. The mixture was then sonicated twice for 30 s each time and centrifuged at 100000*g* for 30 min at 4 °C, and 3−5 mL of lysate was applied to the His-Bind column according to the manufacturer's recommendations (His-Bind Kit, Novagen). After the column was washed with 5 column volumes of washing buffer (His-Bind Kit, Novagen), His-tagged proteins were eluted with 1 M imidazole in 2 mL of elution buffer (His-Bind Kit, Novagen). The eluted samples were exchanged with 10 mM Mopso (pH 7.0), 5 mM $MgCl_2$, and 1 mM DTT using a Centricon-30 apparatus (Amicon, Beverly, MA), and the final samples were adjusted to 50% glycerol before being stored at −20 °C.

*Detection of Cyclase Proteins.* Aliquots of total and soluble (100000*g* supernatant) protein, prepared as described by Back et al. (1994), were separated on an 11.5% SDS−polyacrylamide gel and stained for total protein using Coomassie blue. The stained gels were scanned with a LKB densitometer, and the density of the IPTG inducible band (corresponding to the predicted molecular size for the cyclase protein) was determined as a percentage of the total density scan.

*Enzyme Assay.* The sesquiterpene cyclase assay is based on the amount of radiolabeled hydrocarbon reaction product generated from [$^3$H]FPP that partitions into hexane (Back et al., 1994). Essentially, reactions were quenched by the addition of 0.2 M KOH/0.1 M EDTA and vortexed against an excess volume of hexane to separate labeled hydrocarbon product from [$^3$H]FPP, and after a brief centrifugation (5 s), the radioactivity in an aliquot of the hexane layer was determined by liquid scintillation spectrometry. In a typical assay, 100 $\mu$L of 250 mM Tris-HCl (pH 7.5) containing 50 mM $MgCl_2$, 10 $\mu$M [$^3$H]FPP (50−200 $\mu$Ci/$\mu$mol), and 50 nM enzyme was incubated for 5 min at 30 °C. The reactions were quenched by addition of 100 $\mu$L of quench and extracted with 1.0 mL of hexane.

The stability of products was determined by measuring the radioactivity in both the hexane and aqueous layers following the workup of quenched reaction mixtures that had been incubated at 30 °C for varying periods after the quench. Purified HVS sesquiterpene cyclase (50 nM) was incubated with 10 $\mu$M [$^3$H]FPP (200 $\mu$Ci/$\mu$mol) in a 100 $\mu$L reaction volume for 10 min before addition of 100 $\mu$L of 0.2 M KOH/0.1 M EDTA quench. Quenched samples were maintained at 30 °C for 8−30 min before extraction with 1.0 mL of hexane. Samples of the hexane (200 $\mu$L) and aqueous layers (40 $\mu$L) were transferred to separate scintillation vials and counted. Measurements for each time point were made in duplicate (separate reaction tube). A blank measurement was performed in an identical fashion but with buffer in place of enzyme. The blank was worked up immediately following addition of quench to the reaction mixtures and served as the reference (0 min) time point.

*Steady-State Kinetic Experiments.* Purified cyclases (15−20 $\mu$M) in storage buffer [10 mM Mopso (pH 7.0), 5 mM $MgCl_2$, 1 mM DTT, and 50% glycerol] were diluted with reaction buffer to 100 nM. A portion of the diluted enzyme (50 $\mu$L) was combined with 40 $\mu$L of reaction buffer and allowed to equilibrate to 30 °C for 5 min. [$^3$H]FPP (10 $\mu$L) was added to initiate the reaction. Final concentrations were 50 nM enzyme and 0.6−20 $\mu$M [$^3$H]FPP (200 $\mu$Ci/$\mu$mol), with six concentrations of [$^3$H]FPP tested for each enzyme. Quadruplicate measurements were performed for each [$^3$H]-

FPP concentration. Two of the reactions were quenched after 2 min, and the remaining two were quenched after 4 min (100 $\mu$L quench volume). Mixtures were extracted with 1.0 mL of hexane as described above. The average disintegrations per minute value in aliquots of the hexane phase for the 2 min point was subtracted from the average disintegrations per minute value for that at 4 min, and the result was divided by 2 to obtain the initial reaction velocity in disintegrations per minute. Reactions for each [$^3$H]FPP concentration were initiated, quenched, and extracted with hexane and the mixtures transferred to scintillation vials before proceeding to the next [$^3$H]FPP concentration. Background disintegrations per minute were obtained from reaction mixtures with buffer in place of enzyme and were never larger than 1% of any given reaction disintegrations per minute.

*Pre-Steady-State Kinetic Experiments.* The approach to the steady state of the cyclase-catalyzed reactions was measured using a KinTek rapid mixing apparatus (Johnson, 1995). Experiments were performed in reaction buffer at 30 °C, with enzyme in the first sample loop (14.5 $\mu$L) and [$^3$H]FPP in the second sample loop (14.5 $\mu$L). Final concentrations after mixing were 5.0−50.0 $\mu$M [$^3$H]FPP (200−500 $\mu$Ci/$\mu$mol) and 0.10−1.5 $\mu$M enzyme. Reactions were quenched with 200 $\mu$L of 0.2 M KOH/0.1 M EDTA. The ejected liquid was collected in 13 × 70 mm glass tubes that had been silanized with SigmaCote (Sigma). Duplicate determinations for each time point were obtained by performing successive time course experiments in sequence, in order to eliminate errors due to loss of enzyme activity or inefficient quenching. Quenched reaction mixtures were worked up as described above. The ejected liquid was extracted with 450−900 $\mu$L of hexane and a portion (200−500 $\mu$L) of the extract counted by liquid scintillation spectrometry. Blank reactions were performed in separate Eppendorf tubes with the quench solution added to enzyme before [$^3$H]FPP.

*Rapid Quench Trap Experiments.* Isotope trapping experiments were performed with the rapid mixing apparatus in reaction buffer at 30 °C. Final concentrations after mixing were 12.5 $\mu$M [$^3$H]FPP (400 $\mu$Ci/$\mu$mol) and 0.56 $\mu$M enzyme. The samples were flooded at various reaction times with 200 $\mu$L of 100.0 $\mu$M unlabeled FPP from the center syringe on the apparatus, which reduced the final specific activity of [$^3$H]FPP by 100-fold. The ejected liquid was collected in a 13 × 70 mm silanized glass tube and swirled briefly for 30 s to allow all labeled intermediates to react before 200 $\mu$L of 0.2 M KOH/0.1 M EDTA was added to quench the reaction. The radioactivity in the hydrocarbon products was measured as described above.

*Numerical and Statistical Analysis.* Kinetic constants were determined by a nonlinear regression fit of the pre-steady-state kinetic data to the differential equations associated with the minimal cyclase mechanism (Mathis & Poulter, 1997). The standard error $\delta k_i$ for each kinetic parameter $k_i$ was obtained from the curvature of $\chi^2$ with respect to $k_i$, and the propagation of errors formula was used to obtain standard errors for parameters calculated from fitted parameters (Bevington & Robinson, 1992). In some cases, kinetic parameters were also determined by nonlinear regression fitting to the appropriate analytical expression utilizing Grafit (Erithicus Software, Staines, U.K.).

## RESULTS

*Purification and Characterization of Recombinant Sesquiterpene Cyclases.* In previous work, the steady-state kinetic properties of sesquiterpene cyclase gene products were evaluated using bacterial lysates as the source of the cyclase enzyme, and the reaction products were analyzed by a combination of $Ag^+$-TLC, GC, and GC−MS (Back & Chappell, 1996). Four of the cyclase genes examined in those earlier studies are depicted in Figure 2, along with an indication of their respective reaction products. Both the TEAS and CH3 genes coded for enzymes that catalyzed the accumulation of 5-epi-aristolochene (70% of the total products) and another eremophiliane-type compound (20%). The HVS gene coded for a protein that produced greater than 90% of only the vetispiradiene product. In contrast, the CH4 gene coded for a protein possessing multifunctional activity that gave three reaction products: 18% 5-epi-aristolochene, 43% second eremophiliane-type product, and 32% vetispiradiene.

Although the bacterial lysates were sufficiently active for initial characterization, a detailed kinetic analysis required pure enzymes. We therefore chose to synthesize these enzymes with hexahistidyl-terminal extensions to facilitate their purification (Figure 2A). The constructs were prepared by inserting the full length cyclase genes without stop codons into the pET28(b) expression vector in frame with codons for six additional histidine residues at the carboxyl termini. All four His-tagged constructs directed synthesis of soluble cyclases that were comparable to proteins without the His tags in terms of specific activity and reaction product profiles (data not shown). However, we subsequently discovered that only the CH3, HVS, and CH4 His-tagged cyclases readily bound to the $Ni^{2+}$ affinity column. A further modification of the TEAS construct by fusing the His tag to the amino-terminal portion of the enzyme, as well as attempts to denature and refold the protein, did not improve the recovery of active enzyme from the affinity column. Because the CH3 enzyme activity was identical to that of the TEAS in terms of specific activity and reaction product profile, we therefore focused our subsequent attention on the CH3, CH4, and HVS His-tagged enzymes.

Figure 3 shows the expression level of these three enzymes in *E. coli* as a function of total and soluble protein after induction with IPTG. To determine the relative expression level of the three cyclase proteins in the bacterial lysates, densitometry of the Coomassie blue-stained gels was used to assess the relative abundance of the correctly sized and IPTG inducible cyclase polypeptide. The His-tagged proteins accumulated to 50−60% of the total *E. coli* proteins and represented 35−45% of the soluble protein. On the basis of relative Coomassie blue staining intensities of the proteins separated by SDS−PAGE, a single affinity chromatographic step resulted in purification of the His-tagged proteins to approximately 98% homogeneity (Figure 3, lane 4 for each construct). The yields of the purified enzymes were 5−8% of total soluble protein with increases in specific activities ranging from 85-fold for CH3 to 500-fold for HVS (Table 1).

*Validation of the Enzyme Assay.* Studies with other sesquiterpene cyclases have indicated that the hydrocarbon products of the reaction may be sufficiently volatile at room temperature to bias the assay (Cane et al., 1990b). In a

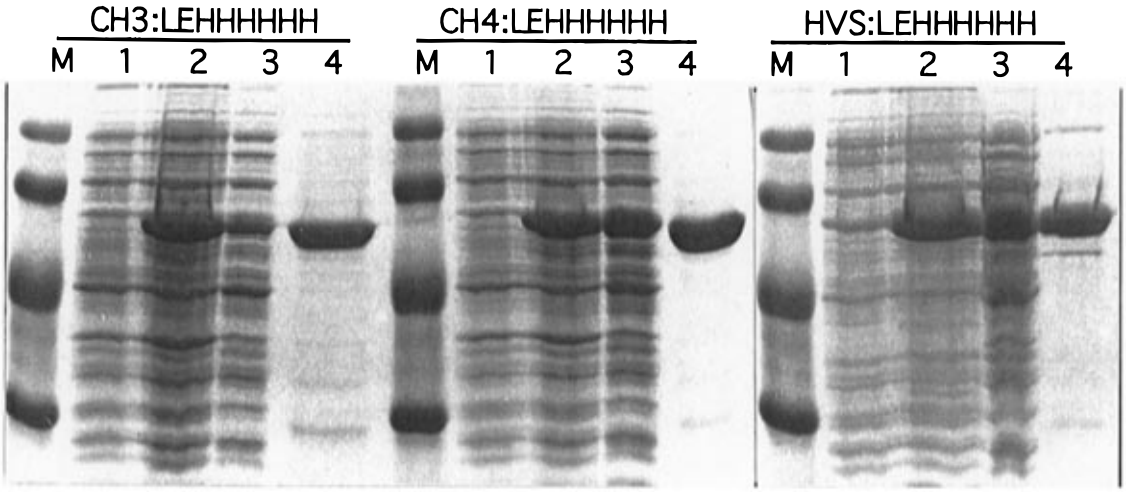


FIGURE 3: Expression of CH3, CH4, and HVS cyclase genes in *E. coli*. Bacteria BL21(DE3) cells harboring either the pET28b-CH3, -CH4, or -HVS cyclase constructs were incubated without or with IPTG before preparing total and soluble protein extracts. Protein samples were separated by SDS−PAGE and stained for total protein using Coomassie blue: M, molecular mass standards (from the top, 110, 70, 43, and 28 kDa); and lane 1, total proteins in 50 $\mu$L aliquots of bacterial culture without IPTG. The pellets were resuspended with 50 $\mu$L of 1× SDS sample buffer [50 mM Tris-HCl (pH 6.8), 10 mM DTT, 2% SDS, 0.01% bromophenol blue, and 10% glycerol]: lane 2, total proteins from IPTG-treated cells; lane 3, 100 $\mu$g of 100000*g* supernatant proteins; and lane 4, cyclase proteins (20 $\mu$g) purified by affinity ($Ni^{2+}$) chromatography.

Table 1: Affinity Purification of Recombinant Sesquiterpene Cyclase Enzymes from Bacteria Expressing pET28b-CH3, -CH4, and -HVS Vector Constructs

| fraction | volume | total protein (mg) | relative activity (nmol $h^{-1}$ $mg^{-1}$) |
|---|---|---|---|
| | CH3-LEHHHHHH | | |
| 100000*g* supernatant | 3 mL | 19.5 | 99 |
| His-Bind ($Ni^{2+}$) column[a] | 800 $\mu$L | 1.0 | 8500 |
| | CH4-LEHHHHHH | | |
| 100000*g* supernatant | 3 mL | 18.6 | 61 |
| His-Bind ($Ni^{2+}$) column[a] | 500 $\mu$L | 1.4 | 11949 |
| | HVS-LEHHHHHH | | |
| 100000*g* supernatant | 5 mL | 35.0 | 35 |
| His-Bind ($Ni^{2+}$) column | 2 mL | 2.0 | 17960 |

[a] Final volume after ultrafiltration using a Centricon-30 apparatus.

control experiment, quenched reaction mixtures from a normal assay were maintained at 30 °C for up to 30 min. Tubes were removed at 5 min intervals and extracted. Portions of the hexane and aqueous layers were counted individually. The decrease in relative disintegrations per minute in the aqueous layer immediately after terminating and extracting the reaction was almost exactly matched by the increase in hexane disintegrations per minute for the first time point. No further change was observed with increasing the time after quench. An additional control experiment was performed in order to determine the necessity (or lack thereof) of drying the extracted hexane with silica before counting. Twenty-four measurements of the disintegrations per minute in the hexane extracts before and after vortexing with 10 mg of silica gave the same result within experimental error. This amount of hexane-soluble impurity in the [$^3$H]-FPP stock was $\leq$1%.

*Steady-State Experiments*. The steady-state constants obtained from initial velocity experiments are presented in Table 2 for each enzyme. Experiments were performed at six concentrations of FPP (0.6−20 $\mu$M) with 50 nM enzyme. Because of a significant burst amplitude associated with 50 nM enzyme, initial velocities were determined from the slope between 2 and 4 min where formation of product was linear.

Table 2: Steady-State Kinetic Constants for Three Recombinant Sesquiterpene Cyclases

| enzymes | $K_{M(FPP)}$ ($\mu$M) | $k_{cat}$ ($s^{-1}$) |
|---|---|---|
| CH3-LEHHHHHH | 0.7 ± 0.4 | 0.04 ± 0.01 |
| CH4-LEHHHHHH | 0.4 ± 0.4 | 0.02 ± 0.01 |
| HVS-LEHHHHHH | 3.5 ± 1.2 | 0.04 ± 0.01 |
| native TEAS enzyme[a] | 2−5 | NR[b] |

[a] Adopted from Vögeli et al. (1990). [b] Not reported.

And, although approximately 40% of the FPP substrate was consumed within 4 min at the lowest FPP concentration (0.6 $\mu$M), the reactions were linear up to this time point. Use of lower concentrations of enzyme (5−10 nM) and longer reaction times resulted in an unsatisfactory degree of scatter in the data. With 50 nM enzyme, HVS and CH3 gave typical Michaelis−Menten initial velocity curves. The individual data points for CH4 showed less curvature, indicating that the concentrations of FPP used in this study were larger than the $K_M$ for CH4. Thus, the $K_M$ value given in Table 2 for CH4 has a proportionately larger standard error than that for either CH3 or HVS. The steady-state constants in Table 2 are typical of those reported for other terpene cyclases (Munck & Croteau, 1990; Zook et al., 1992; Cane, 1990; Cane et al., 1993a; Chen et al., 1995).

*Rapid Quench Experiments*. The pre-steady-state kinetic behaviors of the three cyclases were studied by rapid quench and isotope trapping experiments. The hydrocarbon reaction products corresponded to the sum of enzyme-bound and free species. Three types of pre-steady-state experiments were performed. The first was a rapid quench with KOH/EDTA. In the second experiment, unlabeled FPP was used to trap [$^3$H]FPP released from the E·[$^3$H]FPP complex before catalysis. The third experiment measured the burst rate constant for formation of E·P as a function of FPP concentration. In general, the progress curves in each of the experiments were similar for the three cyclases. Therefore, data are presented only for the CH4 protein, which catalyzes the formation of products reflective of both parent enzymes.

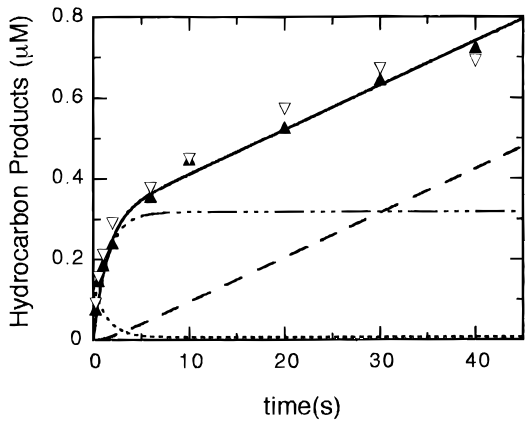


FIGURE 4: Time course for formation of sesquiterpene hydrocarbons by CH4. Concentrations were 12.5 $\mu$M [$^3$H]FPP and 560 nM enzyme. The size of the data points represents the scatter in duplicate determinations. The rapid quench (▲) and isotope trapping (▽) experiments are described in Materials and Methods and Results. The displayed curves are simulated concentrations of intermediates in the reactions ([E·S], ···; [E·P], —···—; [P], − − − ; and [P] + [E·P], —) based on the mechanism in Scheme 1. The integration employed the rate constants compiled in Table 3 and reactant concentrations listed above.

Scheme 1: Minimal Mechanism for the Synthesis of 5-Epi-aristolochene and Vetispiradiene

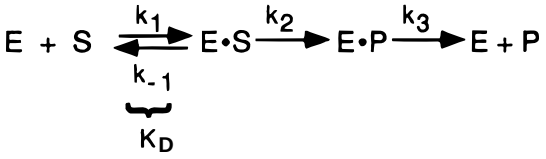


The progress curve obtained for 0.56 $\mu$M CH4 and 12.5 $\mu$M FPP is displayed in Figure 4 (solid points). The size of the displayed data points matches or exceeds the experimental error associated with duplicate determinations. The biphasic curve for formation of radioactive hydrocarbons from FPP indicates that catalysis by CH4 was rate-limited by a step after the initial cyclization of the substrate. Since the assay used in these studies did not permit us to resolve the total hexane-soluble radioactivity into contributions from individual hydrocarbon products, the kinetic data were fit to the simple mechanism shown in Scheme 1 to accommodate the burst profile. In this mechanism, $k_1$ and $k_{-1}$ represent the binding and release steps for formation and dissociation of the enzyme·FPP complex, respectively. There are two possible scenarios for the steps represented by $k_2$ and $k_3$. In one, $k_2$ measures the rate of formation of germacrene A from FPP, and the overall rate-limiting step represented by $k_3$ is either conversion of germacrene A to the final enzyme-bound hydrocarbon product or a step associated with dissociation of the enzyme−product complex. In the other scenario, FPP is rapidly converted to germacrene A; $k_2$ measures the rate of conversion of germacrene A to enzyme-bound product, and $k_3$ represents a product release step. Within these scenarios, the slowest event in the conversion of FPP to germacrene A is most likely the rupture of the carbon−oxygen bond in FPP which forms a high-energy carbocation, and the slowest event in the conversion of germacrene A to the final hydrocarbon product is most likely protonation of the carbon−carbon double bond in germacrene A.

The data were fit to eq 1

$$P_{obs} = P + E{\cdot}P = \alpha[1 - e^{(-\beta t)}] + \gamma t \qquad (1)$$

where $\alpha$ is the apparent burst amplitude, $\beta$ is the reciprocal lifetime of E·P, and $\gamma$ is the steady-state rate, as previously defined in Fersht (1985) and Fierke and Hammes (1995). The fitted values were as follows: $\alpha = 0.34 \pm 0.05$ $\mu$M, $\beta = 0.88 \pm 0.2$ s$^{-1}$, and $\gamma = 0.011 \pm 0.003$ $\mu$M s$^{-1}$. The burst amplitude corresponded to 65% of the concentration of CH4 predicted from a Bradford (1976) assay. The results are consistent with a single catalytic site in CH4 that synthesizes all hydrocarbon products. Variations of enzyme concentration between 0.1 and 1.5 $\mu$M and the interval over which the reaction was monitored from 30 to 60 s did not significantly change the value for $\beta$. Rapid quench experiments carried out with the HVS and CH3 proteins gave time curves that were qualitatively very similar (data not shown) to the curve shown in Figure 4. Enzyme concentrations for CH3 and HVS were from 0.5 to 1.5 $\mu$M, and the concentration of FPP was 25 $\mu$M. As observed for CH4, the apparent burst amplitudes for CH3 and HVS were only ca. 65% of that expected on the basis of the protein concentration determined by the Bradford (1976) assay. These discrepancies may reflect a percentage of inactive enzyme or inaccuracies of the Bradford assay used to measure the level of the sesquiterpene cyclase protein.

Figure 4 also shows the results (open data points) obtained from a trapping experiment where the CH4·[$^3$H]FPP complex was diluted with cold FPP at different time intervals and allowed to stand for 30 s before addition of the KOH/EDTA quench. Substrate concentrations, enzyme concentrations, and time intervals before addition of cold FPP were identical to those used in the rapid quench experiment. This experiment was designed to measure the concentration of enzyme-bound substrate by trapping any [$^3$H]FPP that dissociates from the CH4·[$^3$H]FPP complex. Addition of unlabeled FPP to the CH4·[$^3$H]FPP complex reduced the specific activity of FPP in solution by 100-fold compared to that in the sample loop before initiation of the reaction. Under these conditions, the radioactivity in the products corresponded to

$$P_{obs} = P + E{\cdot}P + f(E{\cdot}S) \qquad (2)$$

where $f(E{\cdot}S)$ denotes the fraction of E·S converted to E·P without dissociation back to free enzyme and substrate.

$$f = \frac{k_2}{k_{-1} + k_2} \qquad (3)$$

As seen in Figure 4, the progress curves for the rapid quench and trapping experiment were virtually identical. Thus, $f(E{\cdot}S)$ in eq 2 was vanishingly small. The most straightforward explanation is that catalysis by CH4 involves an initial, rapid pre-equilibration of free enzyme, substrate, and E·S, and the pre-equilibration is followed by a slower chemical step that precedes the rate-limiting step. A similar experiment was performed with CH3 (data not shown), and comparisons of the progress curves with and without dilution of the specific activity of FPP again showed no differences. Thus, a steady-state concentration of the E·S complex for CH3 was also achieved rapidly relative to chemistry.

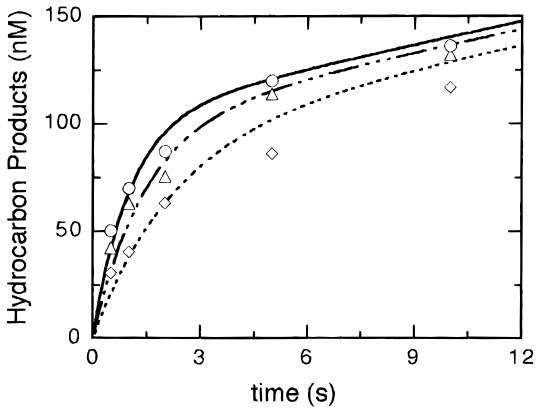


FIGURE 5: Time course for formation of hydrocarbons at different concentrations of FPP, with 190 nM CH4 and 25 (○), 12.5 (△), and 6.25 (◇) $\mu$M FPP. The size of the data points matches or exceeds the scatter observed from duplicate determinations. The displayed curves are simulated observed product concentrations based on the mechanism in Scheme 1, using the rate constants given in Table 3 and enzyme and substrate concentrations listed above.

Figure 5 shows the results of rapid quench experiments for CH4 (190 nM) at three different concentrations of FPP (6.25, 12.5, and 25.0 $\mu$M). These concentrations were found by trial and error to exhibit differences in the burst rate constant ($\beta$ in eq 1), thereby allowing a determination of $K_D$. Equation 4 shows the dependence of $\beta$ on FPP concentration.

$$\beta = \frac{k_2[\text{FPP}]}{K_D + [\text{FPP}]} + k_3 \qquad (4)$$

At the FPP concentrations used in our experiments, $k_3$ is much smaller than the first term and can be neglected. In addition, since the isotope trapping experiment in Figure 4 indicated that $k_{-1} \gg k_2$, $K_D$ appears in eq 4 rather than the more general expression $(k_{-1} + k_2)/k_1$. It is important to emphasize that eq 4 was not employed for the determination of $K_D$; rather, the numerical integration method (see below) was used. [For further discussion about obtaining $K_D$ from burst rate constant experiments, see Johnson (1986) or Dahlberg and Benkovic (1991).] The size of the data points in Figure 5 matches or exceeds the errors observed with duplicate determinations. The time curves were measured only out to the onset of the region of linear product formation. On this time scale, the apparent burst amplitude increased with increasing FPP concentration. A similar experiment with 190 nM HVS and 25, 15, and 7.5 $\mu$M FPP gave progress curves similar to those presented in Figure 5 (data not shown).

The rapid quench data for CH4 in Figures 4 and 5 were combined and fit to the binding mechanism presented in Scheme 1 by numerical integration of the appropriate differential equations. Since the isotope trapping experiments indicated that catalysis was preceded by a fast pre-equilibration of the E·S complex, values for the binding and dissociation rate constants ($k_1$ and $k_{-1}$, respectively) could not be obtained. Therefore, the only parameters varied during the fit were $K_D$, $k_2$, and $k_3$. Integration of the differential equations associated with Scheme 1 was accomplished by arbitrarily setting $k_{-1}$ to 50 $s^{-1}$, which is consistent with the isotope trapping experiment displayed in Figure 4 and with eq 3 ($k_{-1} \gg k_2$). The value for $k_1$ for each iteration was then obtained from $K_D$. The FPP concentrations used were the same as those employed in the experiments and were held constant. Enzyme concentrations were also held constant, taken to be 35% lower than those determined by Bradford (1976) assays. Twenty fitting runs were performed by varying the starting guesses for $K_D$, $k_2$, and $k_3$. In all cases, the same best fit values for $K_D$, $k_2$, and $k_3$ and the minimum value for $\chi^2$ were returned. Initial iteration values for $\chi^2$ were up to 4 orders of magnitude larger than the final, minimum value. Visual inspection of projections of the resultant $\chi^2(K_D,k_2,k_3)$ hypersurface in the neighborhood of the global minimum also gave a measure of the quality of the fit and allowed calculation of standard errors from the curvature of each projection. The combined rapid quench data for HVS were fit using the same procedure. Final values for the kinetic constants are given in Table 3. The values in Table 3 for CH3 were obtained from fits to rapid quench experiments. The curves in Figures 4 and 5 were generated using the parameters in Table 3, assuming values for $k_1$ of $2.9 \times 10^6$ $M^{-1}$ $s^{-1}$ and $k_{-1}$ of 50 $s^{-1}$ that give a $K_D$ equal to the experimentally determined value.

Table 3: Kinetic Constants for Three Recombinant Sesquiterpene Cyclases

| | HVS-LEHHHHHH | CH4-LEHHHHHH | CH3-LEHHHHHH |
|---|---|---|---|
| $K_D$ ($\mu$M) | 69 ± 25 | 18 ± 2.0 | ND[a] |
| $k_2$ ($s^{-1}$) | 0.7 ± 0.2 | 1.6 ± 0.2 | 0.3 ± 0.1 |
| $k_3$[b] ($s^{-1}$) | 0.01 ± 0.03 | 0.04 ± 0.01 | 0.03 ± 0.01 |
| $K_M$[c] ($\mu$M) | 1.0 ± 3.0 | 0.5 ± 0.2 | ND[a] |

[a] Not determined. [b] The catalytic constant is given by $k_{cat} = k_2k_3/(k_2 + k_3)$. Since $k_2 \gg k_3$, $k_{cat} \approx k_3$. [c] Calculated from $K_D$, $k_2$, and $k_3$ according to eq 4 and the propagation of errors formula.

For a simple monoreactant rapid equilibrium Michaelis−Menten mechanism, $K_M = K_D$. This is clearly not the case for HVS and CH4 (see Tables 2 and 3), where $K_M$ for the mechanism shown in Scheme 1 is given by eq 5

$$K_M = \frac{k_3(k_{-1} + k_2)}{k_1(k_2 + k_3)} \approx \frac{k_{-1}}{k_1}\frac{k_3}{k_2} = K_D\frac{k_3}{k_2} \qquad (5)$$

The isotope trapping experiment established that $k_{-1} \gg k_2$, while the rapid quench experiment showed that $k_2 \gg k_3$. Simplification of eq 5 according to these two approximations indicates that $K_M < K_D$ for the cyclases. The values we measured for $K_M$ are in good agreement with those calculated from $K_D$, $k_2$, and $k_3$ (see Table 3) according to the simplified form of eq 5. Values for $k_{cat}$ determined from the pre-steady-state experiments ($k_{cat} \approx k_3$) also agree well with those obtained from the steady-state experiments (see Tables 2 and 3). It is important to note that the steady-state and pre-steady-state experiments were carried out with different preparations of enzyme.

## DISCUSSION

Hohn and Plattner (1989) reported the first heterologous expression of a sesquiterpene cyclase gene in bacteria and noted that the encoded protein, trichodiene synthase, accumulated to only 0.05−0.1% of the total *E. coli* protein. Since that initial report, several improvements and other examples of overexpression of sesquiterpene cyclase genes in bacteria have been reported (Cane et al., 1993a,b; Back

et al., 1994; Chen et al., 1995). Cane and co-workers have emphasized the importance of using a strong, inducible promoter and engineering the gene so that the resulting mRNA contains a proper ribosome binding sequence at its 5′ end to facilitate protein translation. In suitable constructs, they found that aristolochene synthase from *Penicillium roqueforti* (Cane et al., 1993b) and trichodiene synthase from *Fusarium sporotrichioides* (Cane et al., 1993a) accumulated up to 30−40% of the soluble protein in *E. coli*. Several plant sesquiterpene (Back et al., 1994; Chen et al., 1995) and monoterpene (Colby et al., 1993) cyclases have also been produced in bacteria with maximum levels reaching 5−8% of the soluble protein. In the current work, properly engineered plasmids encoding for C-terminal hexahistidyl tags increased overall accumulation of plant cyclases to greater than 50% of the total *E. coli* protein and greater than 35% of the soluble protein. This represents a 5−7-fold improvement over our previous attempts (Back et al., 1994; Back & Chappell, 1995). Addition of a hexahistidyl tag to the cyclases also facilitated their purification with net recoveries of 1−2 mg of 98% pure protein from 100 mL of bacterial culture. Equally important, the hexahistidyl tag did not alter the steady-state kinetic parameters of the enzymes (Vögeli et al., 1990) or the distributions of sesquiterpene products (Back & Chappell, 1996; data not shown).

Our pre-steady-state kinetic analysis implies that all three plant sesquiterpene synthases operate by a rapid equilibration with FPP to form an enzyme−substrate complex, followed by a slightly slower conversion of FPP to hydrocarbons. The rate constants for turnover of the E•P complexes for HVS, CH3, and CH4 are 10−70-fold smaller than those for the initial chemical step. Since our assay was not specific for individual hydrocarbon products, we do not know if the rate-limiting step ($k_3$) is a subsequent chemical transformation, for example protonation of germacrene A, or a nonchemical step such as a conformational change or release of products. To our knowledge, the only other terpene cyclase evaluated in this manner is trichodiene synthase (TS), a fungal sesquiterpene cyclase, which is reported in a companion paper by Cane et al. (1997). These authors report that turnover for fungal TS, like the plant enzymes, is limited by a step following the initial reaction of FPP. A rate-limiting product release step for the terpene cyclases is not unique. For example, turnover for farnesyl diphosphate synthase, an enzyme that catalyzes the basic chain elongation reaction in the isoprenoid pathway, is limited by product release (Laskovics & Poulter, 1981). Also, the kinetic constants obtained for the sesquiterpene cyclases are within the range observed for other slow enzymes (Fersht, 1985).

While the factors that control the regioselectivity of the penultimate rearrangements which lead to 5-epi-aristolochene and vetispiradiene are not clear at the present time, one expects that HVS, CH3, and CH4 all bind FPP in similar conformations to facilitate the initial cyclization of the farnesyl cation to germacrene A. The final selection of aristolochene or vetispiradiene products may well be dictated by subtle differences in the shape or conformation of the active site that slightly alters steric and electronic interactions between the enzyme and the carbocationic sesquiterpene intermediates. This notion is consistent with the conserved biological features in the two enzymes and the similar chemical mechanisms for formation of the two hydrocarbons. The primary sequence of vetispiradiene synthase shares 77% identity with 5-epi-aristolochene synthase (Back & Chappell, 1995), indicative of a common ancestry within the Solanaceae. 5-Epi-aristolochene and vetispiradiene, for example, are formed from FPP by mechanisms that involve several enzyme-bound intermediates (see Figure 1). In the case of 5-epi-aristolochene, the reaction involves rupture of the carbon−oxygen bond in FPP, electrophilic cyclization at C-10 in the distal carbon−carbon double bond, and loss of a proton from a methyl group at C-11 for generation of the ten-membered ring germacrene intermediate (Cane, 1990; Whitehead et al., 1990; Cane & Tsantrizos, 1996). Protonation of a ring double bond in germacrene A, followed by a transannular cyclization, gives the bicyclic eudesmane cation, which then undergoes hydride and methyl shifts before elimination of a proton to form the final product. The route to vetispiradiene follows the same pathway up to the final methyl migration. Instead, an alkyl migration transforms the bicyclic eudesmane skeleton into the isomeric spirocyclic vetispiradiene. Although the combination of electrostatic, dipolar, and conformational effects that lead to regioselectivity for TEAS and HVS is not clear, the peptide substitutions used to construct the CH4 chimera have altered the catalytic site in a manner that reduces stereocontrol and allows the penultimate methyl and alkyl migrations to compete.

## REFERENCES


Back, K., & Chappell, J. (1995) *J. Biol. Chem. 270*, 7375.

Back, K., & Chappell, J. (1996) *Proc. Natl. Acad. Sci. U.S.A. 93*, 6841.

Back, K., Yin, S., & Chappell, J. (1994) *Arch. Biochem. Biophys. 315*, 527.

Bevington, P. R., & Robinson, D. K. (1992) *Data Reduction and Error Analysis for the Physical Sciences*, 2nd ed., McGraw-Hill, New York.

Bradford, M. M. (1976) *Anal. Biochem. 72*, 248.

Cane, D. E. (1985) *Acc. Chem. Res. 18*, 220.

Cane, D. E. (1990) *Chem. Rev. 90*, 1089.

Cane, D. E., & Tsantrizos, Y. S. (1996) *J. Am. Chem. Soc. 118*, 10037−10040.

Cane, D. E., Prabhakaran, P. C., Oliver, J. S., & McIlwaine, D. B. (1990a) *J. Am. Chem. Soc. 112*, 3209.

Cane, D. E., Yang, G., Xue, Q., & Shim, J. H. (1990b) *Biochemistry 29*, 2471.

Cane, D. E., Wu, Z., Oliver, J. S., & Hohn, T. M. (1993a) *Arch. Biochem. Biophys. 300*, 416.

Cane, D. E., Wu, Z., Proctor, R. H., & Hohn, T. M. (1993b) *Arch. Biochem. Biophys. 304*, 415.

Cane, D. E., Yang, G., Xue, Q., & Shim, J. H. (1995) *Biochemistry 34*, 2471.

Cane, D. E., Shim, J. H., Xue, Q., & Fitzimons, B. C. (1995b) *Biochemistry 34*, 2480.

Cane, D. E., Chiu, H.-T., Liang, P.-H., & Anderson, K. S. (1997) *Biochemistry 36*, 8332−8339.

Cassidy, P. B., Dolence, J. M., & Poulter, C. D. (1995) *Methods Enzymol. 250*, 30.

Chandler, J. P. (1976) *QCPE 11*, 307.

Chen, X. Y., Chen, Y., Heinstein, P., & Davisson, V. J. (1995) *Arch. Biochem. Biophys. 324*, 255.

Colby, S. M., Alonso, W. R., Katahira, E. J., McGarvey, D. J., & Croteau, R. (1993) *J. Biol. Chem. 268*, 23016.

Croteau, R. (1987) *Chem. Rev. 87*, 929.

Davisson, V. J., Woodside, A. B., Neal, T. R., Stremler, M. M., & Poulter, C. D. (1986) *J. Org. Chem. 51*, 4768.

Fersht, A. (1985) *Enzyme Structure and Mechanism*, 2nd ed., W. H. Freeman and Co., New York.

Fierke, C. A., & Hammes, G. G. (1995) *Methods Enzymol. 249*, 3.

Guedes, M. E. M., Kuc, J., Hammerschmidt, R., & Bostock, R. (1982) *Phytochemistry 12*, 2987.

Hohn, T. M., & Plattner, R. D. (1989) *Arch. Biochem. Biophys. 275*, 92.

Johnson, K. A. (1986) *Methods Enzymol. 134*, 677.

Johnson, K. A. (1995) *Methods Enzymol. 249*, 38.

Laskovics, F. M., & Poulter, C. D. (1981) *Biochemistry 20*, 1893−1901.

Mathis, J. R., & Poulter, C. D. (1997) *Biochemistry 36*, 6367.

Munck, S. L., & Croteau, R. (1990) *Arch. Biochem. Biophys. 282*, 58.

Sambrook, J., Fritsch, E. F., & Maniatis, T. (1989) *Molecular cloning, A Laboratory Manual*, 2nd ed., Cold Spring Harbor Laboratory Press, Plainview, NY.

Stoessl, A., Stothers, J. B., & Ward, E. W. B. (1976) *Phytochemistry 15*, 855.

Vögeli, U., Freeman, J. W., & Chappell, J. (1990) *Plant Physiol. 93*, 182.

Watson, D. G., & Brooks, C. J. W. (1984) *Physiol. Plant Pathol. 24*, 331.

Wheeler, C. J., & Croteau, R. B. (1987) *Proc. Natl. Acad. Sci. U.S.A. 84*, 4856.

Whitehead, I. M., Threlfall, D. R., & Ewing, D. F. (1989) *Phytochemistry 28*, 775.

Whitehead, I. M., Atkinson, A. L., & Threlfall, D. R. (1990) *Planta 182*, 81.

Zook, M. N., Chappell, J., & Kuc, J. (1992) *Phytochemistry 31*, 3441.

BI963019G